Tellus
SERIES B
CHEMICAL
AND PHYSICAL
METEOROLOGY
PUBLISHED BY THE INTERNATIONAL METEOROLOGICAL INSTITUTE IN STOCKHOLM

Tellus (2010), 62B, 506–511

The space and time impacts on U.S. regional atmospheric CO_2 concentrations from a high resolution fossil fuel CO_2 emissions inventory

By KATHERINE D. CORBIN[1]*, A. SCOTT DENNING[2] and KEVIN R. GURNEY[3]
[1]*Commonwealth Scientific and Industrial Research Organization (CSIRO), Marine and Atmospheric Research, Aspendale, Victoria, Australia*; [2]*Department of Atmospheric Science, Colorado State University, Fort Collins, CO, USA*; [3]*Department of Earth and Atmospheric Sciences, Purdue University, West Lafayette, IN, USA*

(Manuscript received 21 December 2009; in final form 21 June 2010)

ABSTRACT

To improve fossil fuel CO_2 emissions estimates, high spatial and temporal resolution inventories are replacing coarse resolution, annual-mean estimates distributed by population density. Because altering the emissions changes a key boundary condition to inverse-estimated CO_2 fluxes, it is essential to analyse the atmospheric impacts of redistributing anthropogenic emissions. Using a coupled ecosystem–atmosphere model, we compare 2004 atmospheric CO_2 concentrations resulting from coarse and high-resolution inventories. Using fossil fuel CO_2 emissions inventories with coarse spatial and temporal resolution creates spatially coherent biases in the atmospheric CO_2 concentrations. The largest changes occur from using seasonally varying emissions: in heavily populated areas along the west coast and the eastern United States, the amplitude of the near-surface CO_2 concentration seasonal cycle changed by >10 ppm, with higher concentrations in summer and lower concentrations in fall. Due to changes in the spatial distribution, spatially coherent annual mean concentration differences >6 ppm occur; and including the diurnal cycle causes changes >3 ppm. To avoid significant errors in CO_2 source and sink estimates from atmospheric inversions, it is essential to include seasonality in fossil fuel emissions, as well as to utilize higher-resolution, process-based spatial distributions.

1. Introduction

Approximately one-half of the CO_2 emissions from human activities is accumulating in the Earth's atmosphere, whereas the remaining portion of emitted CO_2 is absorbed by sink processes on land and in the ocean (Raupach et al., 2007). Inverse models can be used to quantitatively estimate the strengths and spatial distribution of carbon sources and sinks by combining simulations of atmospheric transport and atmospheric CO_2 concentration data (Enting, 2002). Provided as a boundary condition to the inverse estimation process, accurate fossil fuel emissions are necessary to isolate the biospheric and oceanic fluxes.

Compared with other aspects of the carbon cycle, fossil fuel CO_2 emissions have traditionally been considered well understood. Country-level CO_2 emissions for the industrialized world have been quantified at annual and monthly time scales (Marland and Rotty, 1984, Blasing et al., 2005). To downscale to sub-national spatial scales, Andres et al. (1996, A96) allocated emissions to a $1^\circ \times 1^\circ$ map using political units and population density. Although these estimates are adequate for forward and inverse modelling carbon cycle studies that use coarse spatial scales and annual mean temporal scales, attempts to estimate carbon sources and sinks at finer space (sub-state) and time (sub-month) scales confront several shortcomings: the fossil fuel component lacks seasonal and diurnal variation, has insufficient spatial resolution and uses population density as a spatial proxy, which is not always spatially coincident with fossil fuel combustion. A recent study by Gregg et al. (2009) illustrates that the spatial distribution of emissions is far different than a per capita distribution and that it is essential to include seasonal variations of emissions patterns in modelling studies. In a sensitivity study of atmospheric inversions by Gurney et al. (2005), the lack of seasonality in fossil fuel emissions produced biases of up to 50% of seasonal flux estimates at the height of the growing season in regions where fossil fuel emissions are large.

In an effort to overcome these limitations, Gurney et al. (2009) produced a U.S. process-driven, fuel-specific fossil fuel CO_2 emissions inventory, quantified at scales finer than 10 km h^{-1} for the year 2002. Called the 'Vulcan' inventory (www.purdue.edu/eas/carbon/vulcan/), this data product

* Corresponding author.
e-mail: katherine.corbin@csiro.au
DOI: 10.1111/j.1600-0889.2010.00480.x

includes detail on combustion technology and 48 fuel types through all sectors of the U.S. economy. The Vulcan inventory is built from decades of local/regional air pollution monitoring and complements these data with census, traffic and digital road datasets. The emissions data sets are processed and provided at both the native resolution (geocoded points, county, road, etc.) and on a regularized grid to facilitate atmospheric modelling and climate studies. The Vulcan inventory is being used in energy analysis, socioeconomic studies and forward and inverse atmospheric modelling studies as a replacement for the coarser, population-based fossil fuel estimates (Cragg and Kahn, 2009; Parshall et al., 2009; Schuh et al., 2009). Because the fossil fuel CO_2 emissions are an important boundary condition to the atmospheric CO_2 inversion process and thereby alter the inverse-estimated CO_2 sources and sinks, it is important to understand the impacts of both the spatial distribution and the seasonality of fossil fuel emission on the atmospheric CO_2 concentrations. This study investigates the impact of the Vulcan emissions on CO_2 concentrations using a coupled ecosystem–atmosphere model, SiB3–RAMS.

2. Methods

This study uses the Simple Biosphere Model Version 3 (SiB3) coupled to the Brazilian version of the Colorado State Regional Atmospheric Modeling System (RAMS) (Wang et al., 2007, Corbin et al., 2008). Two year-long SiB3–RAMS simulations over North America are performed for 2004. The simulations use 40 km horizontal grid increments and 46 vertical levels up to 24 km. To cover North America, the simulations have 150 × 90 gridcells. The meteorological fields are initialized and nudged to the National Center for Environmental Prediction (NCEP) meso-scale Eta-212 grid analysis with 40 km horizontal resolution (AWIPS 40-km; Rogers et al., 2000). The initial atmospheric CO_2 field and the lateral boundary concentrations are set and nudged to 3-hourly 2004 global concentrations on a 1.25° × 1° grid from the Goddard Space Flight Center (GSFC) Parameterized Chemical Transport Model (PCTM) (Kawa et al., 2004; Parazoo et al., 2008).

To investigate the impact of spatial and temporal redistribution in fossil fuel emissions on atmospheric CO_2 concentrations, this study utilizes two different inventories: A96 and Vulcan. A96 is a 1° annual distribution of CO_2 emissions from fossil fuel consumption and cement manufacture, and anthropogenic CO_2 was emitted constantly in each grid cell at every time-step. The Vulcan inventory version 1.0 has 10 km horizontal resolution and hourly time-steps over the U.S. domain. Both of the annual fossil fuel CO_2 emissions estimates are re-gridded from their native resolutions to the SiB3–RAMS 40 km grid. Because the simulation is performed for 2004 to utilize the global PCTM CO_2 data set, both the Vulcan and A96 emissions are scaled to match the total estimated 2004 emissions from the Energy Information Administration (EIA, 2007). Neither inventory uses air traffic emissions, and all fluxes are added to the first model layer. The first simulation, FF95, uses A96 fossil fuel emissions estimates; and the second case, HRFF, uses the Vulcan inventory.

3. Results

3.1. Spatial redistribution impacts

To isolate the impact of spatially redistributing fossil fuel emissions, we investigated differences in annual mean CO_2 fluxes and atmospheric CO_2 concentrations. Quantifying the fossil fuel emissions using the Vulcan process-based model rather than using population density redistributes the emissions in space (Fig. 1, top panel). In general, the emissions are reduced over large, spatially coherent areas in the Vulcan inventory. To compensate for this reduction, individual gridcells have much

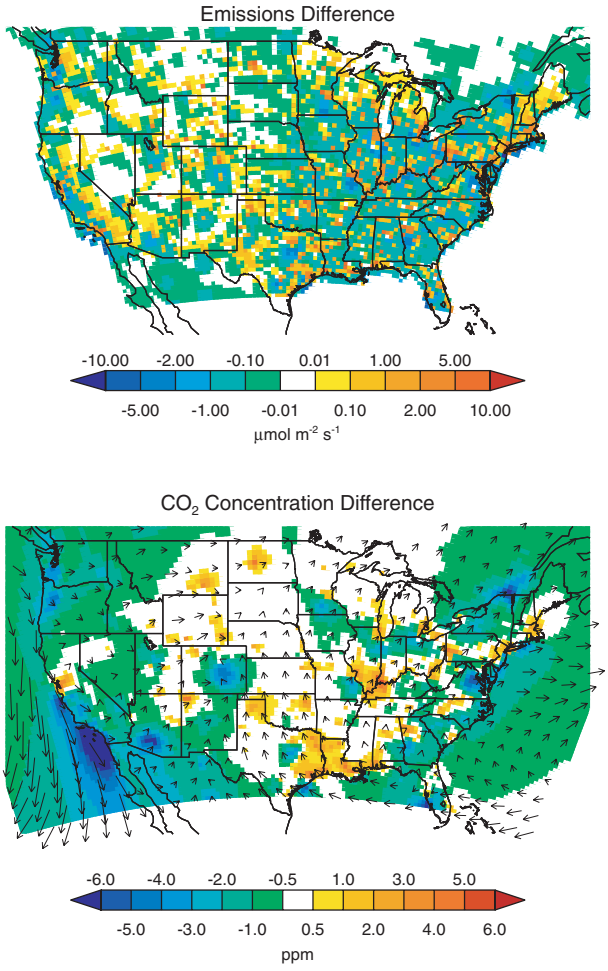

Fig. 1. (Top panel) Difference between A96 annual fossil fuel CO_2 emissions and the Vulcan annual mean estimates (Vulcan—A96). (Bottom panel) Annual mean 30 m CO_2 concentration differences (HRFF—FF95).

higher emissions due to 'point sources' such as power plants or manufacturing facilities. Regional patterns exist where the Vulcan emissions shift from city centres to suburban areas, particularly in the south and east. Differences also occur due to traffic patterns: higher emissions through the central United States correspond to major highways.

Utilization of the higher resolution, process-based emissions inventory versus the population-based approach creates spatially coherent anomalies in the CO_2 concentration field, with differences up to 6 ppm (Fig. 1, bottom panel). The annual mean CO_2 concentration differences reflect the different spatial emission patterns of the two inventories, but are more spatially coherent across large scales when compared to the differences in the surface emissions themselves. The most noticeable differences in the CO_2 concentration field are associated with large point source emission differences. Centres of high concentrations occur in the central and southeastern United States over specific locations of power plants, whereas regions of lower concentrations occur over cities with high-population density but where the power generation does not occur within city limits. Significant changes occur over heavily populated areas in California: the northcentral region has higher concentrations in the HRFF simulation whereas the southern coastline has considerably lower concentrations. The lower concentrations over southern California are advected southward along the coast by strong wind currents, creating a large spatially coherent region over the Pacific ocean. Lower concentrations in the HRFF case also occur over the Pacific northwest, the southwest and the front range of the Rocky Mountains, whereas higher concentrations are seen over the northern-central and southern-central states. Differences due to the spatially coherent emission differences are minimal, due to the small magnitude of the widespread changes.

The alternating patterns of high and low CO_2 creates significant concentration gradients. For example, a gradient of more than 6 ppm occurs in central Texas, where the emissions shift from the city to more remote areas. Several other dipoles of higher and lower concentrations exist throughout the eastern United States, primarily due to shifting of emissions away from population centres to isolated large point sources (e.g. power plants, refineries, large factories).

3.2. *Temporal redistribution impacts*

Fossil fuel emissions vary diurnally and seasonally, and including this temporal variability will impact the resulting atmospheric CO_2 concentrations. On the diurnal time scale, densely populated areas experience maximum emissions during morning and evening rush hours due to heavy motor vehicle traffic. On the seasonal time scale, the United States average Vulcan

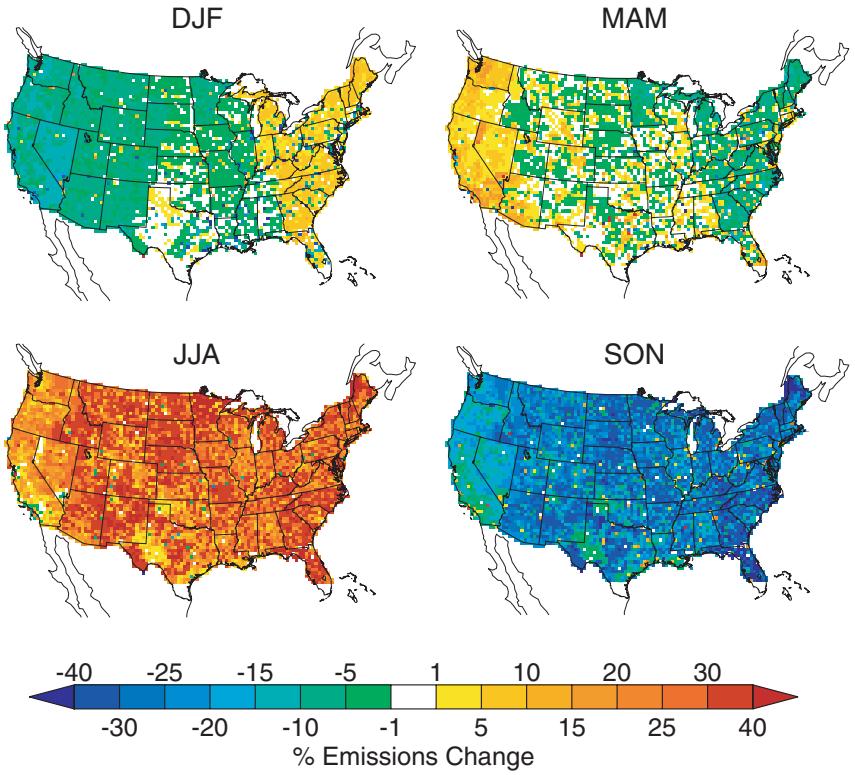

Fig. 2. Seasonal fossil fuel emissions from Vulcan, calculated at every gridcell by subtracting annual mean emission from the 3-month average and then dividing by the annual mean to convert to percent difference for each season.

emissions have maximum emissions in July and August and lower emissions during the spring and fall. The seasonal cycle differs from the long-term mean seasonal cycle reported in Blasing et al. (2005), which showed maximum emissions in January and a secondary maximum in the summer; however, Blasing et al. showed that the magnitude of the summer maximum substantially increased between the 1980s and the 1990s. It should be noted that seasonality in the residential and commercial sectors, which contributed 10% to the total emissions, was not included in the Vulcan release version used in this study.

The seasonal cycle in the Vulcan emissions varies regionally (Fig. 2). Consistent with the U.S. total seasonal cycle, the largest emissions occur during the summer (JJA) and the smallest emissions occur in the fall (SON). Regionally coherent increases (decreases) in fossil fuel emissions persist over the majority of the country during JJA (SON); however, the magnitude of these changes is generally less than 1 μmol m^{-2} s^{-1}, except at localized cities or power plants with large seasonal cycles causing differences greater than 5 μmol m^{-2} s^{-1}. In the winter (DJF) and spring (MAM), the regional seasonality is much weaker, as the differences between the annual mean emissions are generally less than 10% except at individual gridcells. During the first half of the year, the eastern and western halves of the country have opposite anomalies, with the eastern states having higher emissions and the western states generally having lower emissions in DJF (and vice versa for MAM). In general, individual anomalous gridcells (dominated by large point sources or cities) follow the large-scale seasonal cycle; however, the seasonal cycle at several of these locations does vary. For example, in California, individual grid cells with emissions lower and higher than the annual mean can be seen in the summer and fall, respectively. Both large-scale seasonality and individual gridcell seasonality will alter the atmospheric CO_2 concentrations.

Figure 3 shows the CO_2 concentration difference at 30 m above the land surface between the HRFF and FF95 simulations. Spatially coherent differences can be seen in the eastern half of the country, where the concentrations from the HRFF case are higher than the FF95 concentrations in the summer and lower in the fall. The largest difference between the two cases occurs in August, when near-surface CO_2 is more than 15 ppm higher in the HRFF case at individual gridcells. On average, differences spanning 3–6 ppm are seen over the entire eastern portion of the country. In the fall when the Vulcan emissions decrease, the CO_2 concentrations in the HRFF case also decrease, and large-scale differences spanning 4–6 ppm occur in the southeast, with maximum differences in November.

In certain locations, the sign of the differences remains the same throughout the year due to the different spatial allocation of fossil fuel CO_2 emissions in the Vulcan versus A96 data products, but the magnitude of the differences are affected by the Vulcan seasonality. In southern California, lower concentrations persist year-round, but the magnitude of the difference varies

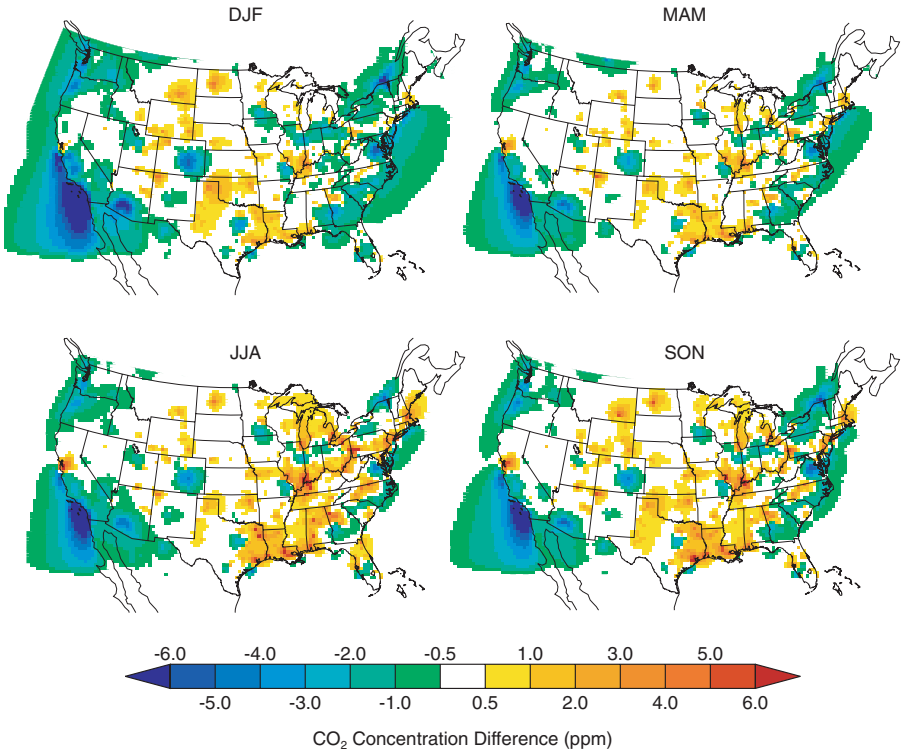

Fig. 3. Seasonal differences in the CO_2 concentrations at 30 m (HRFF—FF95).

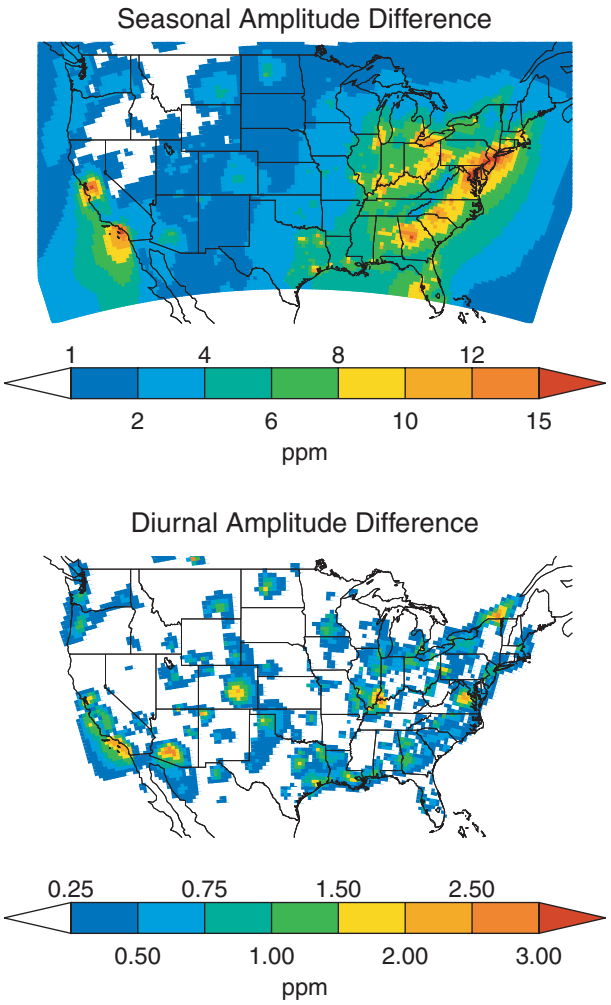

Fig. 4. (Top panel) Seasonal amplitude CO_2 concentration differences at 30 m (HRFF—FF95), where the magnitudes correspond to the amplitudes of spline fits to the CO_2 HRFF—FF95 differences at every grid cell. (Bottom panel) Diurnal amplitude differences at 30 m, calculated by taking the amplitude of the annual mean diurnal cycle from the HRFF—FF95 differences.

from ~6 ppm in the summer to greater than 15 ppm in the fall and winter. Similar features occur across the central states, with spatially coherent differences centred over cities (i.e. Denver, CO and Dallas, TX, USA). Between lower concentrations in the fall and higher concentrations in the summer, the amplitude of the seasonal difference between the HRFF and FF95 simulations exceeds 15 ppm at some locations (Fig. 4, top panel). The magnitudes of the seasonal amplitudes are spatially coherent, highlighting the regions that are significantly affected by the Vulcan seasonality. The seasonal CO_2 amplitudes are greatest over densely populated regions and less dramatic over the central and western United States, where the fossil fuel emissions are smaller.

In addition to seasonal changes, the Vulcan emissions also have diurnal variability. Diurnal variations in emissions cause spatially coherent concentration anomalies over cities and highways; however, the magnitudes of the differences between the two simulations are small relative to the seasonal impacts, causing changes less than 3 ppm (Fig. 4b). Monthly maps of diurnal amplitude concentration differences indicate the seasonal variability in the diurnal cycle only causes small changes in the CO_2 concentration anomalies. Although the diurnal variability does alter the atmospheric concentrations, the impact on regional scales appears to be much smaller than the impacts from seasonally varying emissions.

4. Conclusions

This study investigates the impact on simulated atmospheric CO_2 concentration resulting from the use of Vulcan, a new high-resolution fossil fuel CO_2 emissions inventory created for the United States. When compared to previously used, population-based inventories, the Vulcan emissions show significant spatial and temporal redistribution of the fossil fuel CO_2 sources. When transported with an atmospheric transport model, these space and time emissions differences alter near-surface simulated CO_2 concentrations on regional scales. The different spatial emissions pattern found in the Vulcan inventory creates patterns of alternating high and low CO_2 concentration anomalies that persist over regional scales when compared to CO_2 concentrations driven by the A96 emissions inventory. Including diurnal and seasonal variability in fossil fuel emissions impacts regional CO_2 concentrations on these time scales. Although diurnal impacts appear to be relatively minor, the seasonally varying emissions alter regional concentrations by more than 15 ppm over densely populated regions on the eastern and western coasts. The seasonal impacts are greatest in summer and fall, when the CO_2 concentrations in the HRFF case are generally higher and lower, respectively. The magnitude of the spatial and temporal differences indicates that including fossil fuel seasonality is essential in modelling studies, followed in importance by accurate spatial distribution rather than per capita estimates. Since the use of a high resolution, process driven approach to quantifying fossil fuel CO_2 emissions creates spatially coherent regional-scale anomalies, using coarser spatial distributions with no temporal variability will create biases in the CO_2 concentrations and thus may cause significant errors in source and sink estimates from atmospheric inversions.

5. Acknowledgments

The authors thank Daniel Mendoza and Chris Miller at Purdue University for processing the Vulcan emissions. The authors also thank Rachel Law at CSIRO for very helpful comments and suggestions to the paper. Support for the writing of this work has been granted as part of the Australian Climate Change

Science Program, funded jointly by the Department of Climate Change, the Bureau of Meteorology and CSIRO. This research was funded by NASA under subcontract 521-0438-01 from Purdue University.

References

Andres, R. J., Marland, G., Fung, I. and Matthews, E. 1996. A $1^\circ \times 1^\circ$ distribution of carbon dioxide emissions from fossil fuel consumption and cement manufacture. *Global Biogeochem. Cycles* **10**, 419–429.

Blasing, T. J., Broniak, C. T. and Marland, G. 2005. The annual cycle of fossil-fuel carbon dioxide emissions in the United States. *Tellus* **57B**, 107–115.

Corbin, K. D., Denning, A. S., Lu, L., Wang, J.-W. and Baker, I. T. 2008. Using a high-resolution coupled ecosystem-atmosphere model to estimate representation errors in inversions of satellite CO_2 retrievals. *J. Geophys. Res.-Atmos.* **113**(D02301), doi:10.1029/2007JD008716.

Cragg, M. and Kahn, M. E. 2009. Carbon geography: the political economy of congressional support for legislation intended to mitigate greenhouse gas production. National Bureau of Economic Research Working Paper #14963.

Energy Information Administration. 2007. Emissions of greenhouse gases. In: *Report DOE/EIA-0573*, Office of Integrated Analysis and Forecasting, U.S. Department of Energy, Washington, DC, 64.

Enting, I. 2002. *Inverse Problems in Atmospheric Constituent Transport*. Cambridge University Press, New York, NY.

Gregg, J. S., Losey, L. M., Andres, R. J., Blasing, T. J. and Marland, G. 2009. The temporal and spatial distribution of carbon dioxide emissions from fossil-fuel use in North America. *J. Appl. Met. Clim.* **48**, doi:10.1175/2009JAMC2115.1.

Gurney, K. R., Chen, Y. H., Maki, T., Kawa, S. R., Andrews, A. and co-authors. 2005. Sensitivity of atmospheric CO_2 inversions to seasonal and interannual variations in fossil fuel emissions. *J. Geophys. Res.-Atmos.* **110**(D10308), doi:10.1029/2004JD005373.

Gurney, K. R., Mendoza, D. L., Zhou, Y., Fischer, M. L., Miller and co-authors. 2009. High resolution fossil fuel combustion CO_2 emission fluxes for the United States. *Environ. Sci. Technol.* **43**, doi:10.1021/es900806c.

Kawa, S. R., Erickson III, D. J., Pawson, S. and Zhu, Z. 2004. Global CO_2 transport simulations using meteorological data from the NASA data assimilation system, *J. Geophys. Res.-Atmos.* **109**(D18312), doi:10.1029/2004JD004554.

Marland, G. and Rotty, R. M. 1984. Carbon dioxide emissions from fossil fuels: a procedure for estimation and results for 1950–1982. *Tellus* **36B**, 232–261.

Parazoo, N. C., Denning, A. S., Kawa, S. R., Corbin, K. D., Lokupitiya, R. S. and co-authors. 2008. Mechanisms for synoptic variations of atmospheric CO_2 in North America, South America, and Europe. *Atmos. Chem. Phys.* **8**, 7239–7254.

Parshall, L., Gurney, K. R., Hammer, S. A., Mendoza, D. L., Zhou, Y. and co-authors. 2009. Modeling energy consumption and CO_2 emissions at the urban scale: methodological challenges and insights from the United States, *Energy Policy* **38**(9), doi:10.1016/enpol.2009.07.006.

Raupach, M. R., Marland, G., Ciais, P., Le Quere, C., Canadell, J. G. and co-authors. 2007. Global and regional drivers of accelerating CO_2 emissions. *Proc. Natl. Acad. Sci.* **104**(24), 10288–10293.

Rogers, E., Black, T., Collins, W., Manikin, G., Mesinger, F. and co-authors. 2000. Changes to the NCEP Meso Eta analysis and forecast system: assimilation of satellite radiances and increase in resolution. http://www.emc.ncep.noaa.gov/mmb/mmbpll/eta22tpb.

Schuh, A. E., Denning, A. S., Corbin, K. D., Baker, I. T., Uliasz, M. and co-authors. 2009. A regional high-resolution carbon flux inversion of North America for 2004. *Biogeosci. Discuss.* **6**, 10195–10241.

Wang, J.-W., Denning, A. S., Lu, L., Baker, I. T., Corbin, K. D. and co-authors. 2007. Observations and simulations of synoptic, regional, and local variations in atmospheric CO_2. *J. Geophys. Res,-Atmos.* **112**(D04108), doi:10.1029/2006JD007410.